WEIGHTED COMPACT SCHEME

LI JIANG, HUA SHAN, CHAOQUN LIU
Department of Mathematics
University of Texas at Arlington,
Arlington, Texas, U.S.A.

Abstract.

In this paper a new class of finite difference schemes - the Weighted Compact Schemes are proposed. According to the idea of the WENO schemes, the Weighted Compact Scheme is constructed by a combination of the approximations of derivatives on candidate stencils with properly assigned weights so that the non-oscillatory property is achieved when discontinuities appear. The primitive function reconstruction method of ENO schemes is applied to obtain the conservative form of the Weighted Compact Scheme. This new scheme not only preserves the characteristic of standard compact schemes and achieves high order accuracy and high resolution using a compact stencil, but also can accurately capture shock waves and discontinuities without oscillation. Numerical examples show the new scheme is very promising and successful.

1. Introduction

Recently compact schemes have been widely used in the simulation of complex flows, especially in the direct numerical simulation of turbulent flows (Jiang *et al.*, 1999; Shan *et al.*, 1999; Visbal *et al.*, 1998). Standard finite difference schemes have explicit forms and need to be at least one point wider than the desired approximation order. It is also difficult to find suitable and stable boundary closure for high order schemes. Compared to the standard finite difference approximations, the compact schemes can achieve higher order accuracy without increasing the stencil width. As the compact schemes have implicit forms and involve derivative values of neighboring grid points, additional free parameters can be used not only to improve the accuracy but also to optimize the other properties such as resolution and

stability. The resolution is the largest wave number that can be accurately represented by the scheme. Many complex flows possess a large range of time and space scales. The resolution characteristic of the scheme is essentially important in complex flow simulations. A family of centered compact schemes proposed by Lele (1992) have been proved to have spectral-like resolution. Though the advantages of compact schemes are obvious, there are still difficulties in using them to solve problems involving shock waves or discontinuities. When they are used to differentiate a discontinuous function, the computed derivative has grid to grid oscillation. Compact schemes for filtering are always used together with compact schemes for derivatives to eliminate numerical oscillations (Jiang *et al.*, 1999; Shan *et al.*, 1999; Visbal *et al.*, 1998), but even filtering can not reduce oscillations near the discontinuities. Adams (1996) proposed the hybrid compact-ENO scheme for shock-turbulent interaction problems, in which the upwind-biased compact schemes are coupled with ENO schemes. A detection algorithm is used to identify cells containing large gradients, and then the flux derivative at the faces of such cells is computed with ENO schemes. In this approach, the detecting procedure is very time consuming.

In the present work, a new class of compact schemes which we call the Weighted Compact Schemes, are developed. The building blocks of the Weighted Compact Schemes are the standard compact schemes, which also have centered and biased forms. The Weighted Compact Scheme is a hybrid of different forms of standard schemes. The hybrid idea comes from the WENO schemes (Liu *et al.*, 1994; Jiang *et al.*, 1996). The ENO (Harten *et al.*, 1987; Shu *et al.*, 1988, 1989) and WENO schemes have been applied quite extensively in many different fields. Most of the problems involving shocks, discontinuities and rich structures. The success of the ENO and WENO schemes are so attractive, that the basic methodology inspires the idea of developing the Weighted Compact Scheme. The ENO schemes choose the smoothest stencil to pick one interpolating polynomial for the ENO reconstruction, while the WENO schemes use a convex combination of interpolating polynomials on all candidate stencils to achieve the essentially non-oscillatory property, at the same time additional one order of accuracy is obtained. Thus, WENO schemes remove all the stencil choosing procedures in ENO which is very time consuming. In WENO schemes (Jiang *et al.*, 1996), each of the candidate stencils is assigned a weight that determines the contribution of this stencil to the final approximation of the numerical flux. The weights are defined in such a way that in smooth regions it approaches certain optimal weights to achieve a higher order of accuracy; in regions near discontinuities, the stencils that contain the discontinuities are assigned a nearly zero weight. According to this method, the Weighted Compact Scheme is constructed by the combination of the ap-

proximations of derivatives on candidate stencils. Here the finite difference approximations of derivatives are combined together to form a new finite difference approximation, while in WENO schemes interpolating functions are combined. The general idea of the Weighted Compact Scheme is the following, on each candidate stencil, for a given accuracy order, there is a corresponding finite difference compact scheme. According to the smoothness of each stencil, a weight is assigned to each finite difference approximation obtained by compact schemes. The hybrid of these standard schemes, with corresponding weights, forms the new scheme - the Weighted Compact Scheme. The weights are defined in such a way that the stencils, including discontinuities, have less contribution to the final scheme. Thus, the oscillations near discontinuities can be avoided, while high order accuracy and high resolution properties of compact schemes can still be preserved in the smooth region.

Another problem while using compact schemes is the conservation property of the schemes. Conservation property is especially important in solving problems involving shocks. Nonconservative methods usually generate large errors near the shock. Lele (1992) developed conservative formulations of the finite difference compact scheme by constructing the near boundary schemes in such a way that the discrete form of global conservation is satisfied. This approach is applicable when the scheme coefficients are constant. Davis (1998) applied the primitive function reconstruction method of ENO schemes to a compact scheme to maintain the conservation. In the present work, this method is applied with the new scheme to achieve the conservation.

In section 2 the general idea of the Weighted Compact Scheme is described in detail. The method of applying the new scheme in a conservative form is given. In section 3 we apply the new scheme to solving several typical equations. The problems involving shocks, discontinuities and fine structures are simulated. The numerical results are given.

2. Weighted Compact Scheme

2.1. BASIC FORMULATION

For simplicity, we consider a uniform grid. The independent variable at the node j is $x_j = h(j-1)$ for $1 \leq j \leq N$ and the function value at the nodes $f_j = f(x_j)$ is given. The finite difference approximation f'_j to the first derivative of the function f on the nodes can be written in the following general form while the finite difference compact scheme (Lele, 1992) is used.

$$\beta_- f'_{j-2} + \alpha_- f'_{j-1} + f'_j + \alpha_+ f'_{j+1} + \beta_+ f'_{j+2}$$

$$= \frac{1}{h}(b_- f_{j-2} + a_- f_{j-1} + c f_j + a_+ f_{j+1} + b_+ f_{j+2}) \tag{1}$$

For a given point j, three candidate stencils containing this point are defined as follows:

$$S_0 = (x_{j-2}, x_{j-1}, x_j), \quad S_1 = (x_{j-1}, x_j, x_{j+1}), \quad S_2 = (x_j, x_{j+1}, x_{j+2}).$$

On each stencil a finite difference compact scheme is derived in the form of Eq.(1) by matching the Taylor series coefficients to various orders. When the following coefficients are used:

$$\begin{aligned}
&S_0: \quad \beta_- = \vartheta,\ \alpha_- = 2\vartheta + 2,\ b_- = -\tfrac{5}{2}\vartheta - \tfrac{1}{2},\ a_- = 2\vartheta - 2,\ c = \tfrac{1}{2}\vartheta + \tfrac{5}{2};\\
&S_1: \quad \alpha_- = \tfrac{1}{4},\ \alpha_+ = \tfrac{1}{4},\ a_- = -\tfrac{3}{4},\ a_+ = \tfrac{3}{4},\ c = 0;\\
&S_2: \quad \beta_+ = \vartheta,\ \alpha_+ = 2\vartheta + 2,\ b_+ = \tfrac{5}{2}\vartheta + \tfrac{1}{2},\ a_+ = -2\vartheta + 2,\ c = -\tfrac{1}{2}\vartheta - \tfrac{5}{2},
\end{aligned} \tag{2}$$

where ϑ is a free parameter. In this work, we set $\vartheta = 0$ to get a tridiagonal form. This parameter can also be used to improve the accuracy or optimize the scheme. The sacrifice would be increase the computer time. Those coefficients which are not listed are set to zero. Then, the schemes corresponding to stencils S_0 and S_2 are third order one-sided finite difference schemes, and the scheme corresponding to S_1 is a fourth order centered scheme. As compact schemes have implicit forms, each scheme is represented by an equation in the form of Eq.(1) with coefficients defined in (3) . These three equations are denoted as F_0, F_1, F_2. Then a specific weight is assigned to each equation, and a new scheme is obtained by a summation of the equations.

$$F = C_0 F_0 + C_1 F_1 + C_2 F_2 \tag{3}$$

where, C_0, C_1, C_2 are weights and satisfy $C_0 + C_1 + C_2 = 1$. If the weights are properly chosen, the new scheme can achieve a higher order accuracy because the additional free parameters are introduced. If we set:

$$C_0 = C_2 = \frac{1}{18 - 24\vartheta}, \quad C_1 = \frac{8 - 12\vartheta}{9 - 12\vartheta} \tag{4}$$

the new scheme given by Eq. (3) is at least a sixth order centered compact scheme. The procedure described above implies that the sixth order centered compact scheme can be represented by a combination of three lower order schemes.

Obviously, the scheme F is a standard finite difference compact scheme and cannot avoid the oscillation near discontinuities. In order to achieve non-oscillatory property, the method of the WENO scheme (Jiang *et al.*,

1996) is introduced to determine the new weight for each stencil. The weights are determined according to the smoothness of the function on each stencil. Following the WENO method, the new weights are defined as (Jiang *et al.*, 1996):

$$\omega_k = \frac{\gamma_k}{\sum_{i=0}^{2} \gamma_i} \quad \gamma_k = \frac{C_k}{(\epsilon + IS_k)^p} \tag{5}$$

where ϵ is a small positive number which is used to prevent the denominator becoming zero. p is an important parameter to control the weight. At present time, it is set as a constant. IS_k is the smoothness measurement which is defined according to WENO (Jiang *et al.*, 1996):

$$\begin{aligned} IS_0 &= \frac{13}{12}(f_{j-2} - 2f_{j-1} + f_j)^2 + \frac{1}{4}(f_{j-2} - 4f_{j-1} + 3f_j)^2 \\ IS_1 &= \frac{13}{12}(f_{j-1} - 2f_j + f_{j+1})^2 + \frac{1}{4}(f_{j-1} - f_{j+1})^2 \\ IS_2 &= \frac{13}{12}(f_j - 2f_{j+1} + f_{j+2})^2 + \frac{1}{4}(f_{j+2} - 4f_{j+1} + 3f_j)^2 \end{aligned} \tag{6}$$

where, the two terms on the right side can be regarded as the measurements of the curvature and the slope respectively at a certain point. Through the Taylor expansion, it can be easily proved that in smooth regions new weights ω_k satisfy:

$$\omega_k = C_k + O(h^2) \ \ and \ \ \omega_2 - \omega_0 = O(h^3). \tag{7}$$

The new scheme is then formed using these new weights:

$$F = \omega_0 F_0 + \omega_1 F_1 + \omega_2 F_2. \tag{8}$$

The leading error of F is also a combination of the errors of the original schemes F_i, which is as following:

$$(\frac{1}{12}\omega_0 - \frac{1}{12}\omega_2) f^{(4)} h^3 + (-\frac{1}{15}\omega_0 + \frac{1}{120}\omega_1 - \frac{1}{15}\omega_2) f^{(5)} h^4. \tag{9}$$

When Eq. (7) is satisfied, the leading error of the new scheme can be written as $O(h^6)$. Obviously, this new scheme is of sixth-order accuracy and has the high resolution property as the centered sixth-order compact scheme in smooth regions. But in the regions containing discontinuities, the smoothness measurement IS_k of the non-smooth stencil is large compared to that of the smooth stencil, thus the non-smooth stencil is assigned a small weight and have less contribution to the final scheme so that the non-oscillatory property is achieved.

With the new weights ω_k, the new finite difference compact scheme Eq. (8) is written in the form of Eq. (1). The coefficients of the final Weighted Compact Scheme are given as follows:

$$\beta_- = \vartheta\omega_0,\ \alpha_- = (2\vartheta+2)\omega_0 + \frac{1}{4}\omega_1,$$
$$\alpha_+ = (2\vartheta+2)\omega_2 + \frac{1}{4}\omega_1,\ \beta_- = \vartheta\omega_2,$$
$$b_- = (-\frac{5}{2}\vartheta - \frac{1}{2})\omega_0,\ a_- = (2\vartheta-2)\omega_0 - \frac{3}{4}\omega_1,$$
$$c = (\frac{1}{2}\vartheta + \frac{5}{2})\omega_0 - (\frac{1}{2}\vartheta + \frac{5}{2})\omega_2,$$
$$a_+ = (-2\vartheta+2)\omega_2 + \frac{3}{4}\omega_1,\ b_+ = (\frac{5}{2}\vartheta + \frac{1}{2})\omega_2.$$

As ω_k is dependent on the smoothness measurement calculated by local function values, the scheme coefficients are various from point to point. The free parameter ϑ can be used to optimize the scheme when the properties of high resolution, and stability are concerned. If $\vartheta = 0$, the scheme is tridiagonal. Though in the above description the sixth-order Weighted Compact Scheme is selected as an example, the method can be extended to a general form.

2.2. CONSERVATIVE FORMULATION

The conservation property of the scheme is very important in shock wave capturing, since it imposes a constraint on the solution error. In the work of Davis (1998), the reconstruction method developed by Shu and Osher (1989) for the ENO scheme was used together with the Pade scheme to achieve the conservation. As we already mentioned in the previous section, the coefficients of our new scheme are not constant. So the finite difference scheme itself is not conservative. However, conservation can be obtained when the Weighted Compact Scheme is applied together with ENO reconstruction method. Below, we give the description of this method. For 1-D conservation laws:

$$u_t(x,t) + f_x(u(x,t)) = 0. \tag{10}$$

When a conservative approximation to the spatial derivative is applied, a semi-discrete conservative form of Eq. (10) is as follows:

$$\frac{du_j}{dt} = -\frac{1}{\Delta x}\left(\hat{f}_{j+\frac{1}{2}} - \hat{f}_{j-\frac{1}{2}}\right), \tag{11}$$

$\hat{f}_{j+\frac{1}{2}}$ and $\hat{f}_{j-\frac{1}{2}}$ are numerical flux functions at the cell interfaces. Δx is the grid size of the uniform grid. In order to achieve the high order accuracy, the numerical flux should be defined in such a way that the difference of the numerical flux is a high order approximation of the derivative f_x. According to the ENO reconstruction procedure (Shu *et al.*, 1989), it has been approved that the primitive function of $\hat{f}$ at the cell interfaces can be exactly calculated by the given point values f_j. If H is the primitive function of $\hat{f}$, then:

$$H(x_{j+\frac{1}{2}}) = \Delta x \sum_{i=-\infty}^{j} f_i. \tag{12}$$

Obviously, the numerical flux $\hat{f}$ at the cell interfaces is the derivative of its primitive function H. i.e:

$$\hat{f}_{j+\frac{1}{2}} = H'_{j+\frac{1}{2}}. \tag{13}$$

As the values of the function H have already been obtained at the cell interfaces, the approximations of the derivatives of H at the cell interfaces are calculated directly by the Weighted Compact Scheme presented in Section 1. Thus, the Weighted Compact Scheme is applied to the primitive function instead of the function itself. In this way, the conservation property is achieved.

3. Numerical Examples

The prospects of the Weighted Compact Scheme can be seen from our applications of the tridiagonal sixth-order scheme described in section 1 to some model equations and test examples. According to our experience, when the reconstruction method is adopted, the function f in Eq.(10) is used to define the smoothness IS_k instead of using primitive function H. The parameter p in Eq. (5) is set as $p = 1$. For all of the following examples, the fourth order Runge-Kutta scheme (Shu *et al.*, 1988) is used for time integration.

3.1. CONVECTION EQUATION

We first solve the one-dimensional convection equation with several initial functions.

$$\begin{aligned} &u_t + u_x = 0, \qquad -1 \le x \le 1 \\ &u(x,0) = u_0(x), \qquad \textit{periodic with a period of } 2. \end{aligned} \tag{14}$$

N	L_∞ error	L_∞ order	L_1 error	L_1 order
20	4.39E-5		1.19E-5	
40	1.05E-6	5.38	2.37E-7	5.64
80	2.70E-8	5.28	4.23E-9	5.81
160	5.94E-10	5.50	6.35E-11	6.05
320	1.14E-11	5.70	7.15E-13	6.47

TABLE 1. Errors of the numerical solution with $u_0(x) = sin(\pi x)$ at $t = 1$, Weighted Compact Scheme

N	L_∞ error	L_∞ order	L_1 error	L_1 order
20	1.48E-5		9.46E-6	
40	2.26E-7	6.03	1.44E-7	6.02
80	3.57E-9	5.98	2.27E-9	5.98
160	5.88E-11	5.92	3.74E-11	5.92
320	1.07E-12	5.78	5.73E-13	6.02

TABLE 2. Errors of the numerical solution with $u_0(x) = sin(\pi x)$ at $t = 1$, Standard Compact Scheme

The first initial function is $u_0(x) = sin(\pi x)$. The second one is $u_0(x) = sin^4(\pi x)$. The L_1 and L_∞ errors are listed in Table 1 to Table 3. N is the number of grid points. Table 1 and 2 are the results for the first initial function and are obtained respectively by the Weighted Compact Scheme and the standard compact scheme. This data shows that the Weighted Compact Scheme is capable of achieving sixth-order accuracy as the standard compact scheme. Table 3 lists the result for the second initial function. Compared to the results (Jiang *et al.*, 1996) obtained by WENO scheme, this Weighted Compact Scheme achieves higher order accuracy with the same stencils.

The third to fifth initial functions are:

$$(3)\quad u_0(x) = \begin{cases} 1, & -\frac{1}{5} \le x \le \frac{1}{5}; \\ 0, & otherwise, \end{cases}$$

N	L_∞ error	L_∞ order	L_1 error	L_1 order
20	3.73E-2		1.16E-2	
40	4.54E-3	3.03	1.17E-3	3.31
80	5.37E-4	3.07	5.54E-5	4.04
160	7.08E-6	6.25	7.98E-7	6.12
320	4.84E-8	7.19	6.99E-9	5.98
640	2.65E-10	7.51	7.61E-11	6.52

TABLE 3. Errors of the numerical solution with $u_0(x) = sin^4(\pi x)$ at $t = 1$

$$(4)\quad u_0(x) = \begin{cases} \left[1 - (\frac{10}{3}x)^2\right]^{\frac{1}{2}}, & -\frac{3}{10} \le x \le \frac{3}{10}; \\ 0, & otherwise, \end{cases}$$

$$(5)\quad u_0(x) = e^{-300x^2}.$$

Figure 1 is the result of the standard compact scheme for the initial function (3). The solution is seriously damaged by wiggles generated near the discontinuities. Figures 2-4 illustrate the results obtained by the Weighted Compact Scheme for initial functions (3), (4), and (5). There is no obvious numerical oscillation observed in the regions near the discontinuities, and good resolution has been achieved.

3.2. BURGERS' EQUATION

The Weighted Compact Scheme is applied to the nonlinear Burgers' equation. With the given initial condition, the exact solution will develop to a moving shock wave.

$$u_t + (\frac{1}{2}u^2)_x = 0, \qquad -1 \le x \le 1 \tag{15}$$

$$u(x,0) = \frac{1}{2} + sin(\pi x), \qquad periodic\ with\ a\ period\ of\ 2.$$

At $t = 0.15$ the solution is still smooth. The L_∞ and L_1 errors are listed in Table 4. The scheme also has about sixth-order accuracy for the nonlinear problem.

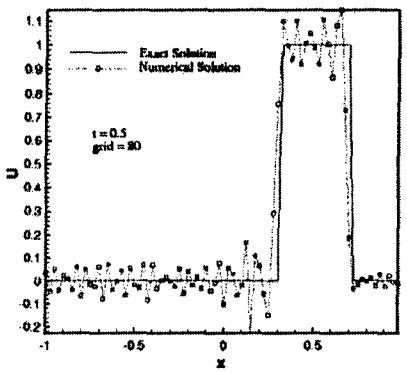

Figure 1. Solution of standard compact scheme

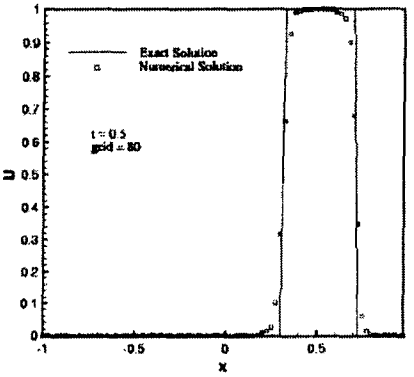

Figure 2. The solution at $t = 0.5$

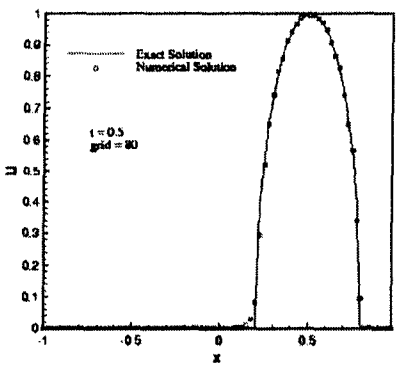

Figure 3. The solution at $t = 0.5$

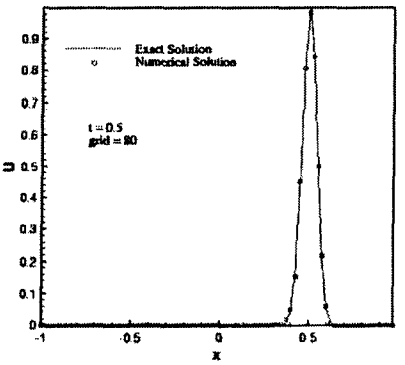

Figure 4. The solution at $t = 0.5$

N	L_∞ error	L_∞ order	L_1 error	L_1 order
80	4.45E-5		3.63E-6	
160	1.75E-6	4.67	4.85E-8	6.23
320	4.41E-8	5.31	9.49E-10	5.85

TABLE 4. Errors of the numerical solution of Burgers' equation. $t = 0.15$

Fig. 5 and Fig. 6 show the wave at $t = 0.3183$ and $t = 0.55$. At $t = 0.3183$ the wave becomes steep and the shock starts to form. At $t = 0.55$ the discontinuity appears and is accurately captured by the scheme without obvious oscillation.

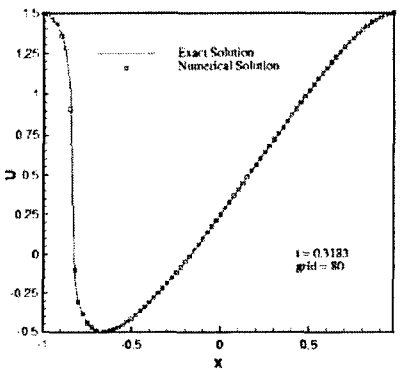

Figure 5. The solution to the Burgers' equation at $t = 0.3138$

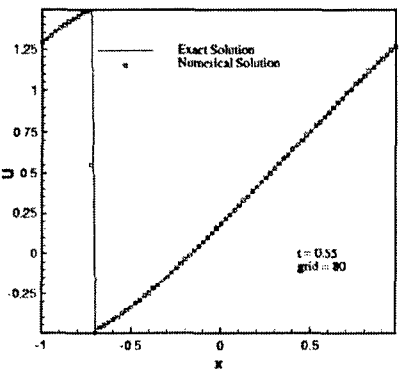

Figure 6. The solution to the Burgers' equation at $t = 0.55$

3.3. 1D EULER EQUATION

We apply our scheme to 1D Euler equation of gas dynamics

$$\begin{aligned} &\frac{\partial U}{\partial t} + \frac{\partial F}{\partial x} = 0 \\ &U = (\rho, \rho u, E)^T \\ &F = (\rho u, \rho u u + p, u(E + p))^T. \end{aligned} \tag{16}$$

The first example is the typical one-dimensional shock tube problem. The initial conditions are chosen so that the solution contains a shock, contact discontinuity and a rarefraction wave. They are given as follows:

$$U_0 = \begin{cases} (1, 0, 1), & x < 0; \\ (0.125, 0, 0.1), & x \geq 0, \end{cases}$$

The distributions of pressure, density,velocity and energy are shown in Fig. 7. The shock wave and contact discontinuity are accurately captured.

The second example is to simulate the interaction between shock wave and fluctuations. The calculation starts with the initial field as follows:

$$U_0 = \begin{cases} (3.857143, 2.629369, 10.33333), & x < -4; \\ (1 + 0.2sin(5x), 0, 1), & x \geq -4. \end{cases}$$

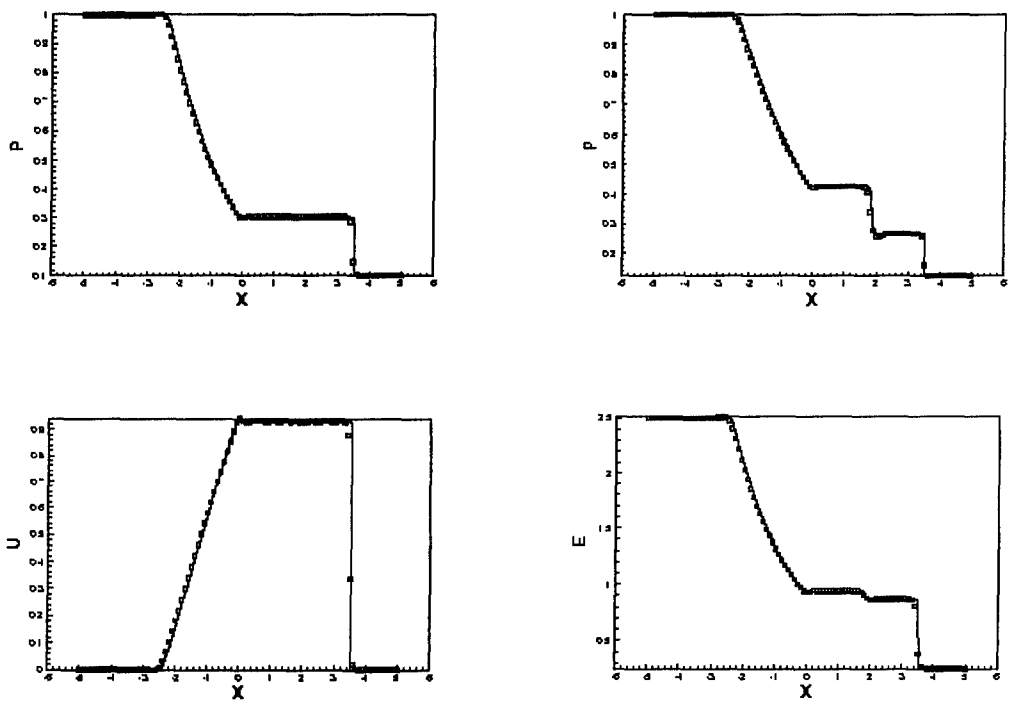

Figure 7. The solutions to the shock-tube problem at $t = 2$, $N = 100$

In this example, the shock is moving into a density fluctuation field and interacts with the fluctuation. This problem requires non-oscillatory scheme with high resolution to resolve the fine structures. In Fig. 8, the solid line represents the numerical solution obtained using the present scheme with a fine grid of $N = 1600$. This is regarded as the exact solution. The results obtained with $N = 400$ compared well with the exact solution. These results show that the present schemes are capable of resolving fine structures with high frequency. No serious oscillation appears near the shock area.

3.4. 2D EULER EQUATION

Finally, we apply the Weighted Compact Scheme to investigate a 2D shock-turbulence interaction problem(Adams,1996; Shu,1989). 2D Euler equations are written as

$$\frac{\partial U}{\partial t} + \frac{\partial F}{\partial x} + \frac{\partial G}{\partial y} = 0 \tag{17}$$

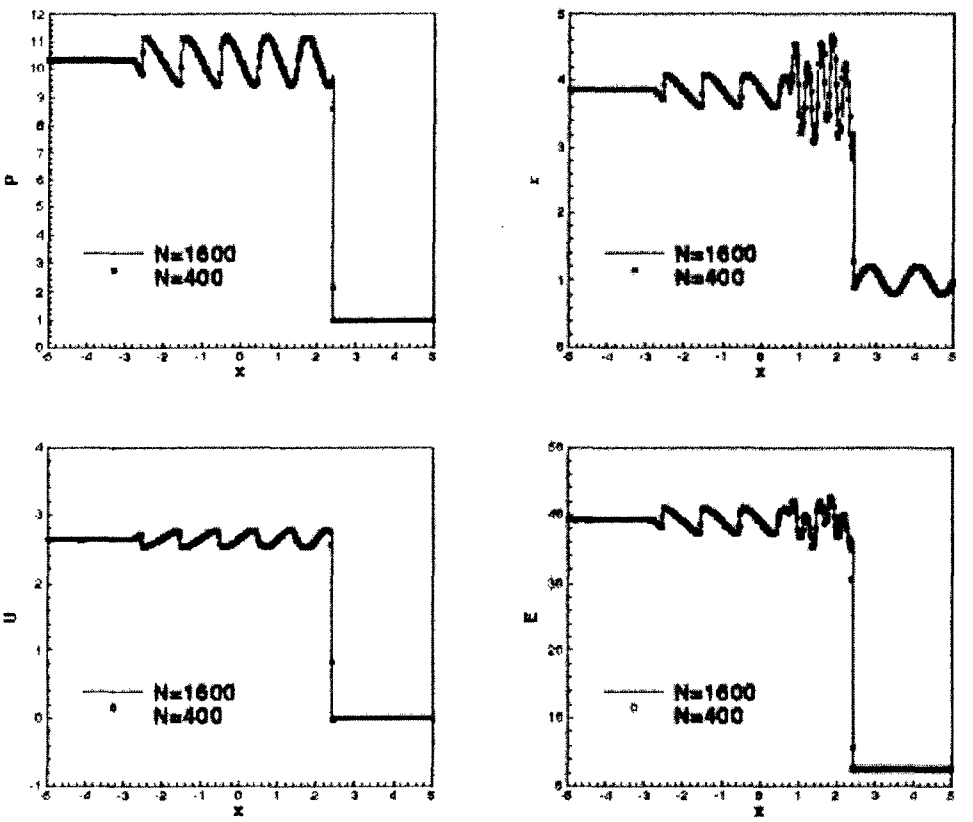

Figure 8. The solutions to the shock-fluctuation interaction problem at $t = 1.8$, $N = 400$

$$U = (\rho, \rho u, \rho v, E)^T$$
$$F = (\rho u, \rho uu + p, \rho uv, u(E + p))^T$$
$$G = (\rho u, \rho vu, \rho vv + p, v(E + p))^T$$

where $E = \frac{p}{\gamma - 1} + \frac{1}{2}\rho(u^2 + v^2)$. The computational domain is given by $-1.5 < x < 1.5$, $-1 < y < 1$. At time $t = 0$, a Mach 8 shock at $x = -1$ is moving in the positive x direction into a vorticity fluctuation field. The initial condition for pre-shock field is specified with vorticity fluctuation as

$$u_1 = -c_1 sin\theta cos(xkcos\theta + yksin\theta)$$
$$v_1 = c_1 cos\theta cos(xkcos\theta + yksin\theta)$$
$$\rho_1 = 1$$
$$p_1 = 1$$

where c_1 is the speed of sound, $k = 2\pi$, $\theta = \frac{1}{6}$. The initial post-shock state can be derived from shock relations.

$$u_2 = \frac{2(M_s^2 - 1)}{(\gamma + 1)M_s^2} u_s$$
$$v_2 = 0$$
$$\rho_2 = \frac{(\gamma + 1)M_s^2}{2 + (\gamma - 1)M_s^2} \rho_1$$
$$p_2 = (1 + \frac{2\gamma(M_s^2 - 1)}{\gamma + 1}) p_1$$

where $u_s = M_s c_1$ is the shock propagation velocity, and M_s is the shock Mach number.

Fig.3.4-3.4 display the results obtained on different grids. The shock front is clearly shown by the pressure contour lines. After the vorticity fluctuations strike the shock, the shock front develops ripples and the vorticity fluctuations are amplified. The results are similar compared with those obtained by Shu (1989) and Adams (1996). This example shows again that the Weighted Compact Scheme can be used for shock-turbulence interaction problems.

4. Conclusions

The conservative Weighted Compact Scheme developed in this work has been successfully applied to several one dimensional typical problems involving discontinuities, shock waves, and shock-fluctuation interaction. High order accuracy, high resolution, and non-oscillation are achieved by using compact stencil. This new scheme will be further applied to multi-dimensional flows with shock-turbulence interactions.

Acknowledgments

This work was supported by Air Force Office of Scientific (AFOSR) research grant monitored by Dr. L. Sakell and Dr. Thomas Beutner. The authors are grateful for AFOSR's sponsorship of this research work. The authors also would like to thank DoD HPCC for providing computer resources.

References

1. Adams, N.A. and Shariff, K., (1996), A high-resolution hybrid compact-ENO scheme for shock-turbulence interaction problems, *J. Comput. Phys.*, **127**, pp.27-51.
2. Davis, S. F., (1998), Shock capturing with Pade method, *Applied Mathematics and Computation*, **89**, pp.85-98.
3. Harten, A., Engquist, B., Osher, S. and Charavarthy, S., (1987), Uniformly high order accurate essentially non-oscillatory scheme, III, *J. Comput. Phys.*,**71**, pp.231-303.

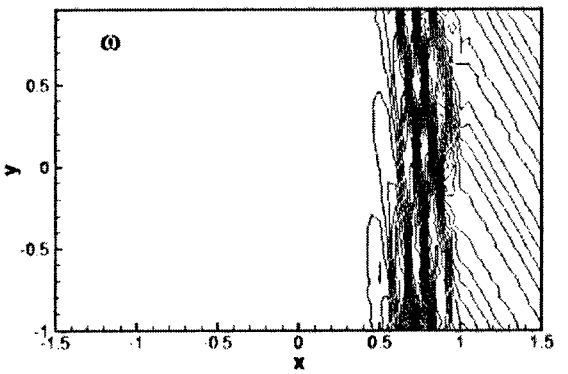

Contours of vorticity

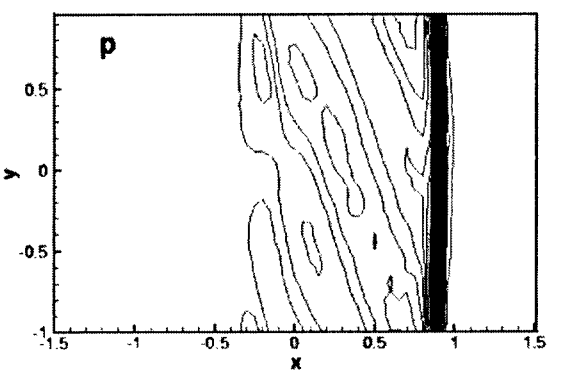

Contours of pressure

Figure 9. Grid=60 × 40,t=0.2

4. Jiang, G. S. and Shu, C. W., (1996), Efficient implementation of weighted ENO scheme. *J. Comput. Phys.*, **126**, pp.202-228.
5. Jiang, L., Shan, H. and Liu, C., (1999), Direct numerical simulation of boundary-layer receptivity for subsonic flow around airfoil, *The Second AFOSR International Conference on DNS/LES*, Rutgers, New Jersey, June 7-9.
6. Lele, S. K., (1992), Compact finite difference schemes with spectral-like resolution. *J. Comput. Phys.*, **103**, pp.16–42.
7. Liu, X. D., Osher, S. and Chan, T., (1994), Weighted essentially non-oscillatory schemes, *J. Comput. Phys.*, **115**, pp.200-212.
8. Shan, H., Jiang, L., Zhao, W. and Liu, C., (1999), Large eddy simulation of flow transition in a supersonic flat-plate boundary layer. *AIAA Paper* 99-0425.
9. Shu, C. W. and Osher, S., (1988), Efficient implementation of essentially non-oscillatory shock-capturing schemes , *J. Comput. Phys.*, **77**, pp.439-471.
10. Shu, C. W. and Osher, S., (1989), Efficient implementation of essentially non-oscillatory shock-capturing schemes II, *J. Comput. Phys.*, **83**, pp.32-78.

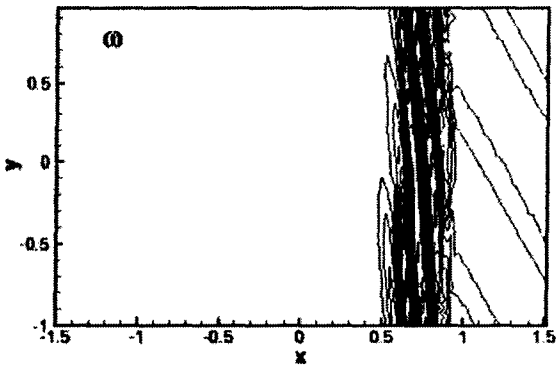

Contours of vorticity

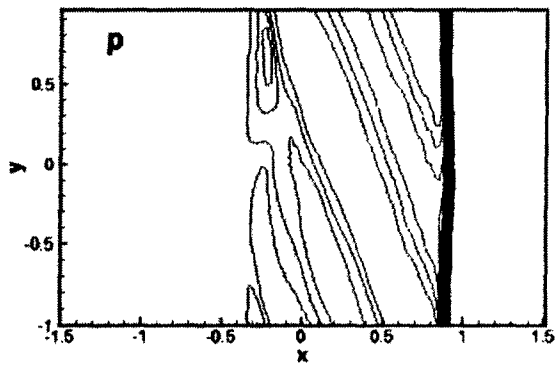

Contours of pressure

Figure 10. Grid=120 × 80,t=0.2

11. Visbal, M. R. and Gaitonde, D. V., (1998), High-order accurate methods for unsteady vortical flows on curvilinear meshes, *AIAA Paper* 98-0131.